Chance-Constrained Generic Energy Storage Operations under Decision-Dependent Uncertainty

Ning Qi, *Student Member, IEEE,* Pierre Pinson, *Fellow, IEEE,* Mads R. Almassalkhi, *Senior Member, IEEE,* Lin Cheng, *Senior Member, IEEE,* and Yingrui Zhuang, *Student Member, IEEE,*

***Abstract*—Compared with large-scale physical batteries, aggregated and coordinated generic energy storage (GES) resources provide low-cost, but uncertain flexibility for power grid operations. While GES can be characterized by different types of uncertainty, the literature mostly focuses on decision-independent uncertainties (DIUs), such as exogenous stochastic disturbances caused by weather conditions. Instead, this manuscript focuses on newly-introduced decision-dependent uncertainties (DDUs) and considers an optimal GES dispatch that accounts for uncertain available state-of-charge (SoC) bounds that are affected by incentive signals and discomfort levels. To incorporate DDUs, we present a novel chance-constrained optimization (CCO) approach for the day-ahead economic dispatch of GES units. Two tractable methods are presented to solve the proposed CCO problem with DDUs: (1) a robust reformulation for general but incomplete distribution of DDUs and (2) an iterative algorithm for specific and known distribution of DDUs. Furthermore, reliability indices are introduced to verify the applicability of the proposed approach with respect to the reliability of GES units' response. Simulation-based analysis shows that the proposed methods yield conservative, but credible GES dispatch strategies and reduced penalty cost by incorporating DDUs in the constraints and leveraging data-driven parameter identification. This results in improved availability and performance of coordinated GES units.**

***Index Terms*—generic energy storage, chance-constrained optimization, decision-dependent uncertainty, response reliability**

I. Introduction

The high penetration of renewable energy resources (RES) gives rise to challenges associated with frequency and voltage regulation, power system stability, and reliability [1]. Deterministic dispatchable resources, such as conventional power plants (CPP) and physical energy storage (ES), have been widely used to overcome these challenges. However, relying on these deterministic resources may not be viable in the future. First, the number of fossil fuel power plants will decrease dramatically due to carbon dioxide emission reduction targets [2], [3]. Second, direct control of a myriad of ES assets within different sectors (e.g., industrial, residential, etc.) will be costly and unlikely. Thus, demand response (DR) and other forms of dispatchable distributed resources represent a less costly alternative and can support reliable power system operations. Such flexibility may be leveraged and controlled via price-based [4] or incentive-based [5] mechanisms. Significant effects on risk hedging and economic operation have been reported [4]–[6], via optimal control of energy usage of thermostatically controlled load (TCL), electric vehicle (EV), and battery energy storage (BES). Most of distributed energy resources have the attributes and abilities of ES devices, hence motivating the term "virtual energy storage" (VES) [7]. In this paper, ES and VES are considered under a common framework called generic energy storage (GES) to unify modeling and uncertainty descriptions of both an individual GES unit and a portfolio of GES units.

The literature related to the modeling and economic dispatch (ED) of GES is vast. Early research mainly focused on modeling and dispatching the flexibility of GES from diverse, responsive loads [7]–[9]. Among these works, a virtual battery model is introduced in [9] and describes how to obtain the GES parameters from TCL assets by using first-order energy dynamics, but without considering time-varying and stochastic features. However, the main difference between GES and conventional ES is the inherent exogenous and endogenous uncertainties of the former [10]. Exogenous uncertainties are uncertainties triggered by factors external to the system and are also called decision-independent uncertainties (DIUs), as they are independent of the operation and control strategy (e.g., uncertainties related to the outputs of RES). Probabilistic optimization of GES under diverse DIUs have been widely investigated in past works and generally considers uncertainty around power and energy capacities and response probability of GES, which is derived from a combination of the following: (i) forecast error of ambient space (temperature) [11], (ii) DR duration [12] and customers' comfort [13], (iii) economic effect driven by incentive or price [4], and (iv) model reduction error [14] and SoC estimation error [15]. For these studies, the structure of DIUs can be fully determined in advance with complete information of uncertainties. However, some stochastic properties may practically be affected by decision variables/control strategies and thus be denoted as decision-dependent uncertainties (DDUs). For instance, the response probability of a GES unit will likely decrease with increased DR frequency, magnitude, and duration [10]. And the magnitude and duration of discomfort can beget manual overrides and result in reduced capacity of a GES [16]. These relations are generally overlooked or simplified away as static and known probability distributions.

Technically speaking, DDUs are divided into two distinct types, which we will refer to as Type 1 and Type 2 [17]. For Type 1-DDUs, decisions influence the parameter realizations by altering the underlying probability distributions for the uncertain parameters. In contrast, for Type 2-DDUs, decisions influence the parameter realizations by affecting the timing or content of the information we observe. Type 2-DDUs have been addressed in long time-scale planning problems using, e.g., multi-stage stochastic optimization with adequately defined scenario trees [18]. For fast time-scale GES op-

N. Qi, L. Cheng, and Y. Zhuang are with State Key Laboratory of Control and Simulation of Power Systems and Generation Equipment, Department of Electrical Engineering, Tsinghua University, 100084 Beijing, China (e-mail: qn18@mails.tsinghua.edu.cn). P. Pinson is with the Department of Technology, Management and Economics, DTU Denmark Technical University, 2800 Kgs. Lyngby, Denmark (e-mail: ppin@dtu.dk). M. Almassalkhi is with the Department of Electrical and Biomedical Engineering, University of Vermont, Burlington, VT 05405 USA and Otto Mønsted Visiting Professor with DTU Center for Electric Power and Energy (e-mail: malmassa@uvm.edu) and acknowledges support from the U.S. National Science Foundation (NSF) Award ECCS-2047306. This paper was sponsored by National Key R&D Program of China (Grant No. 2018YFC1902200) and the project of National Natural Science Foundation of China (Grant No. 52037006 & No. 51807107)

erations described herein, DDUs can be simplified as Type 1-DDUs. Though DDUs are rarely discussed in the literature, the following relevant methods exist today for DDUs: (i) robust optimization (RO) and (ii) stochastic optimization (SO). The assumption of linear decision-dependency of polyhedral uncertainty sets on decision variables is considered in [19], [20], rendering a static RO-DDUs model. Adaptive RO-DDUs models that incorporate wait-and-see decisions and endogenous uncertainties are studied in [21], [22], where an iterative algorithms was employed to handle the computational challenge raised by the coupling relationship between uncertainties and decisions in two stages. Ref. [23] reformulates the problem into multi-stage SO based on a scenario tree. The related works indicate that the key to the optimization under DDUs is to decouple decisions and uncertainty description through iterative algorithms. However, these methods are subject to simplified linear modeling of DDUs that guarantee convergence. To ensure accurate characterization of GES performance [24] and consideration for complex decision-dependent customer behavior dynamics [16], it becomes necessary to incorporate DDUs with nonlinear (but convex) structure. Furthermore, to satisfy decision-makers with different risk preferences and assess the reliability performance of GES units, chance-constrained optimization (CCO) may be preferred relative to SO and RO. To the best our knowledge, no research work has concurrently modeled DDUs of GES in the CCO framework and provided a feasible approach to optimization under non-linear (convex) structure of DDUs with possibly unknown underlying probability distributions.

To fill in the research gap in both modeling and solution methodologies, this manuscript addresses the day-ahead chance-constrained economic dispatch of GES with a modified baseline model within which both DIUs and DDUs can be considered, thus, providing a general framework for optimization of GES. Specifically, the main contributions of this manuscript are threefold:

i) Modeling: We propose a modified baseline model and detailed uncertainty description with DIUs and DDUs of GES. Compared with the model from [9], the proposed GES model incorporates time-varying and rate-limited properties and considers four common device types where parameters can be obtained by a data-driven approach [14]. For the uncertainty description, we consider three types of DIUs (on-off state probability, parameter identification errors and uncertain baseline consumption) and two types of DDUs (available SoC bounds affected by incentive price and response discomfort).

ii) Methodology: Two tractable reformulations are proposed to effectively solve the CCO with DDUs by decoupling decisions and uncertainties. For DDUs with general but incomplete knowledge of distribution, a robust approximation approach is introduced to obtain conservative results based on the maximum value of the unknown inversed CDF, by different versions of Cantelli's inequality. For specific distribution of DDUs, an iterative algorithm allows reducing the optimality gap, while using the robust approximation value as a starting point. The iterative algorithm is also guaranteed to converge to the optimum within a nonlinear (convex) DDU framework.

iii) Numerical study: We introduce two reliability indices, *loss-of-response probability* and *expected response energy not served* to assess the effectiveness and practicality of different strategies and the consequence of overlooking various types of DIUs and DDUs from literature. The case study shows that the proposed models and methods substantially outperform previous approaches in terms of the response reliability due to (1) reduced incomplete knowledge of DIUs via data-driven parameter identification, (2) incorporating DDUs in constraints, which effectively reduces the penalty cost of response losses and improves availability and performance of coordinated GES units.

The remainder of the paper is organized as follows. The modified baseline model of GES is proposed in Section II. Uncertainty modeling with DIUs and DDUs is presented in Section III. CCO under DIUs and DDUs, as well as two reformulation methods, are proposed in Section IV. Numerical studies based on real-world data are provided in Section V to illustrate comparative performance. Extensions of the proposed model are discussed in Section VI. Finally, conclusions are summarized in Section VII.

II. Baseline Model of Generic Energy Storage

The basic model of GES initially presented in [9] is extended herein for four types of commonly used energy resources, i.e., BES, inverter air-conditioner (IVA), and fixed-frequency air-conditioner (FFA), and EV. This manuscript extends the basic GES model to incorporate time-varying and ramp-rate properties as shown in (1a)-(1f). Constraint (1a) defines the relationship between charging and discharging actions, SoC, and additional energy input terms from baseline consumption. The newly-introduced constraint (1b) limits the charging/discharging ramp rates on changes in SoC while constraint (1c) represents time-varying upper and lower bounds on SoC. Constraint (1d) ensures a sustainable energy state for the GES over time. Constraints (1e) - (1f) limit the upper and lower charging and discharging actions. Since sufficient conditions are satisfied (i.e., charging price ("-") is lower than discharging price ("+"), the complementary constraint for charging and discharging is relaxed and has been removed from model [25].

GES Constraints: $\forall t \in \mathbf{\Omega}_T$, $\forall i \in \mathbf{\Omega}_S$

$$SoC_{i,t+1} = (1-\varepsilon_i) SoC_{i,t} + \eta_{\mathrm{c},i} P_{\mathrm{c},i,t} \Delta t / S_i - P_{\mathrm{d},i,t} \Delta t / (\eta_{\mathrm{d},i} S_i) + \alpha_{i,t} \tag{1a}$$

$$-SoC_{i,\mathrm{RD}} \le SoC_{i,t+1} - SoC_{i,t} \le SoC_{i,\mathrm{RU}} \tag{1b}$$

$$\underline{SoC}_{i,t} \le SoC_{i,t} \le \overline{SoC}_{i,t} \tag{1c}$$

$$SoC_{i,T} = SoC_{i,0} \tag{1d}$$

$$0 \le P_{\mathrm{c},i,t} \le \overline{P}_{\mathrm{c},i,t} \tag{1e}$$

$$0 \le P_{\mathrm{d},i,t} \le \overline{P}_{\mathrm{d},i,t} \tag{1f}$$

In the above, $\mathbf{\Omega}_T$ and $\mathbf{\Omega}_S$ are sets of time periods and GES units, respectively. Subscripts *i* and *t* define GES unit and time period, respectively. Decision variables $P_{\mathrm{c},i,t}$ and $P_{\mathrm{d},i,t}$ are the charge, discharge power, which are the additional power actions besides the baseline consumption $P^{\mathrm{B}}_{i,t}$. Variables $SoC_{i,t}$ and Δt define SoC and time-step. Parameters $\overline{P}_{\mathrm{c},i,t}$ and $\overline{P}_{\mathrm{d},i,t}$ are the maximum charge and discharge ratings, respectively, while $\overline{SoC}_{i,t}$ and $\underline{SoC}_{i,t}$ are the upper and lower SoC bounds, respectively. Up and down ramp rate for changes in SoC are given by $SoC_{i,\mathrm{RU}}$ and $SoC_{i,\mathrm{RD}}$. Parameters $\eta_{\mathrm{c},i}$ and $\eta_{\mathrm{d},i}$ are the charge and discharge efficiency, while ε_i and S_i are the self-discharge rate and energy capacity. The newly introduced $\alpha_{i,t}$ are specialized for TCL and EV as the additional SoC changes from baseline consumption.

The relationship between modeling parameters and physical parameters of each energy resource type is summarized in Table I. Thermal capacity, thermal resistance, and conversion efficiency of TCL are given by C, R, and η, while T^{in} and T^{out} define

the indoor and outdoor temperature. These parameters can be obtained by data-driven methods (i.e., load decomposition and parameter identification) [14]. The transformation of TCLs into GES begins with the thermodynamics of a 1^{st} order equivalent thermal parameter (ETP) model, and the difference between IVA and FFA lies in the control mode and power property The proof of the transformation of a TCL and EV to a GES is provided in [26]. Note that the different device types can beget different GES parameters. For instance, the self-discharge rate ε is usually ignored for BES, but is not negligible for other GES types. In addition, most of the parameters are constant for a BES, but time-varying for other GES types, e.g., power and SoC bounds, addition SoC changes: $\varepsilon SoC_t^{\mathrm{B}}$ for TCLs and $\Delta SoC_t^{\mathrm{B}}$ for EVs.

TABLE I
MAPPING GES MODEL PARAMETERS TO PHYSICAL RESOURCES

GES model parameters	Physical BES	Physical TCL (IVA/FFA)	Physical EV
SoC_t	SoC_t	$\frac{\overline{T}^{\mathrm{in}} \quad T_t^{\mathrm{in}}}{\overline{T}^{\mathrm{in}} \quad \underline{T}^{\mathrm{in}}}$	SoC_t
$\overline{P}_{\mathrm{c},t}$	$\overline{P}_{\mathrm{c}}$	$\overline{P} \quad P_t^{\mathrm{B}}$	$\overline{P}_{\mathrm{c}} \quad P_{\mathrm{c},t}^{\mathrm{B}}$
$\overline{P}_{\mathrm{d},t}$	$\overline{P}_{\mathrm{d}}$	$P_t^{\mathrm{B}} \quad \underline{P}$	$\overline{P}_{\mathrm{d}} \quad P_{\mathrm{d},t}^{\mathrm{B}}$
$\underline{SoC}_t$	$\underline{SoC}$	$\frac{\overline{T}^{\mathrm{in}} \quad \overline{T}_t^{\mathrm{in}}}{\overline{T}^{\mathrm{in}} \quad \underline{T}^{\mathrm{in}}}$	$\underline{SoC}_t$
$\overline{SoC}_t$	$\overline{SoC}$	$\frac{\overline{T}^{\mathrm{in}} \quad \underline{T}_t^{\mathrm{in}}}{\overline{T}^{\mathrm{in}} \quad \underline{T}^{\mathrm{in}}}$	$\overline{SoC}_t$
ε	ε	$1 \quad e^{-\Delta t/RC}$	ε
S	S	$\frac{\Delta t(\overline{T}^{\mathrm{in}} \quad \underline{T}^{\mathrm{in}})}{\eta R \varepsilon}$	S
$\eta_{\mathrm{c/d}}$	$\eta_{\mathrm{c/d}}$	1	$\eta_{\mathrm{c/d}}$
α_t	0	$(1 \quad e^{-\Delta t/RC}) SoC_t^{\mathrm{B}}$	$\Delta SoC_t^{\mathrm{B}}$

III. UNCERTAINTIES IN GES OPERATIONS

To capture the effect of exogenous and endogenous uncertainties, this section defines three types of DIUs and two type of DDUs in operations of GES. While the results are general, we use TCL to guide discussions.

A. Three types of decision-independent uncertainties

(a) On-off State Probability (DIU, Single Time)

GES units usually only respond to DR commands when in on-state. Under conventional operations, local control logic defines the on-off transitions, which means that a GES unit is not always responsive to DR commands. Thus, the probability distribution of on-off state $\omega_{i,t}$ can be modeled as a Bernoulli distribution:

$$f(\omega_{i,t}) = \begin{cases} p_{i,t} & \omega_{i,t}=1 \\ 1-p_{i,t} & \omega_{i,t}=0 \end{cases}, \forall t \in \boldsymbol{\Omega}_T, \forall i \in \boldsymbol{\Omega}_S \tag{2}$$

i.e., with the on-state probability $p_{i,t}$ (for unit *i* and time *t*) obtained from historical data. This DIU clearly affects the reliability of the response of GES units.

(b) Parameter Identification Errors (DIU, Single Time)

Identification errors of GES parameters (e.g., $R, C, \overline{T}^{\mathrm{in}}, \underline{T}^{\mathrm{in}}, T_0^{\mathrm{set}}, \overline{P}, \underline{P}$ for TCL assets)are inherent to the process since we employ a simple low-order, lumped model that ignores higher-order realities. As shown in [14], the identification errors depend strongly on the quality of data used but are generally within $\pm 10\%$. Parameter identification errors can be modeled with a truncated normal distribution:

$$\xi_i \sim \mathcal{N}(\mu_{\xi_i}, \sigma_{\xi_i}, a_{\xi_i}, b_{\xi_i}), \forall \xi_i \in \boldsymbol{\Omega}_E, \tag{3}$$

where ξ_i is a random parameter, e.g., for a TCL model, and the TCL parameters are given by $\boldsymbol{\Omega}_E = \{R_i, C_i, \overline{T}_i^{\mathrm{in}}, \underline{T}_i^{\mathrm{in}}, T_{i,0}^{\mathrm{set}}, \overline{P}_i, \underline{P}_i\}, \forall i \in \boldsymbol{\Omega}_S$. The mean and standard deviation of parameters are given by μ_{ξ_i} and σ_{ξ_i}, and ξ_i lies within interval $[a_{\xi_i}, b_{\xi_i}]$. This DIU mainly affects GES power and SoC bounds shown in Table I.

(c) Uncertain baseline consumption (DIU, Single Time)

The distribution of GES baseline consumption can be determined from historical data and modeled with a lognormal distribution:

$$P_{i,t}^{\mathrm{B}} \sim \mathcal{LN}(\mu_{P_{i,t}^{\mathrm{B}}}, \sigma_{P_{i,t}^{\mathrm{B}}}), \forall t \in \boldsymbol{\Omega}_T, \forall i \in \boldsymbol{\Omega}_S. \tag{4}$$

The mean and standard deviation of baseline consumption are denoted by $\mu_{P_{i,t}^{\mathrm{B}}}$ and $\sigma_{P_{i,t}^{\mathrm{B}}}$, while the baseline SoC is denoted by $SoC_{i,t}^{\mathrm{B}}$ and related with baseline consumption. This DIU mainly affects the power bounds of GES units.

As shown, DIU(a)-(c) can capture different exogeneous uncertainties, however, to characterize endogenous uncertainties we present two types of DDUs next.

B. Two types of decision-dependent uncertainties

(a) Available SoC bounds Expansion Effect Driven by Incentive Price (DDU, Single Time) and (b) Contraction Effect Driven by Response Discomfort (DDU, Across Time)

The ability of a GES to actively deliver grid services with sufficient capacity levels is another important uncertainty to consider. Physically, SoC is bounded by *known* limits that satisfy $SoC_t \in [0,1]$ as marked with blue lines in Fig. 1. In addition, the *available* bounds of SoC are strictly contained within the interval $(0,1)$ and time-varying, due to the uncertain baseline consumption (i.e., DIU (b-c)). This is illustrated in Fig. 1 in green rainbow lines.

However, incentives and discomfort will further affect the available SoC bounds, which comes as a trade-off between discomfort (i.e., disutility sustained during grid services) and expected earnings (i.e., incentives or prices) from managing a GES. Thus, the available SoC bounds are dependent on (past) grid service commands. Specifically, the decision-dependent bounds will *expand* and *contract* based on incentive payments and discomfort, respectively, as shown with red rainbow lines in Fig. 1. In particular, the response of a GES to a specific incentive or discomfort is uncertain and begets DDUs.

Thus, a general structure that characterizes these two opposing DDUs (i.e., expansion and contraction) is presented next in (5):

$$\overline{SoC}_{i,t}^{\mathrm{DDU}} = h(g(\overline{SoC}_{i,t}^{\mathrm{DIU}}, c_{\mathrm{c},i,t}^{\mathrm{S}}),\ \beta_i^{\mathrm{U}} RD_{i,t}) \tag{5a}$$

$$\underline{SoC}_{i,t}^{\mathrm{DDU}} = h(g(\underline{SoC}_{i,t}^{\mathrm{DIU}}, c_{\mathrm{d},i,t}^{\mathrm{S}}),\ \beta_i^{\mathrm{L}} RD_{i,t}) \tag{5b}$$

$$RD_{i,t} = \lambda \sum_{\tau=1}^{t} \left(P_{\mathrm{c},i,\tau}/\overline{P}_{\mathrm{c},i} + P_{\mathrm{d},i,\tau}/\overline{P}_{\mathrm{d},i}\right)/T + (1-\lambda)\max\{|SoC_{i,t} - SoC_{i,t}^{\mathrm{B,av}}| - SoC_{i,t}^{\mathrm{DB}}/2, 0\}, \tag{5c}$$

where g is a non-decreasing function of the GES incentive payment (charging/discharging prices, $c_{\mathrm{c/d},i,t}^{\mathrm{S}}$) and represents the expanded

SoC bounds without contraction effects. Function h is monotonically decreasing in response discomfort $RD_{i,t}$ associated with different discomfort-aversion factors, $\beta_i^{\mathrm{L}} \geq \beta i^{\mathrm{U}} \geq 0$. The GES discomfort is modeled in (5c) as a weighted normalized function of disutility and discomfort. The right part of equation represents the relative response intensity affecting disutility, while the right-most part describes the absolute deviation of actual SoC from average baseline SoC, which is inspired by the symmetric thermostat of a TCL centered by the comfortable status. This function can be generalized by incorporating a discomfort deadband, $SoC_{i,t}^{\mathrm{DB}}$, around the average baseline SoC, $SoC_{i,t}^{\mathrm{B,av}}$ within which no discomfort is accumulated. The bounds of deadband is named as comfortable SoC bounds (i.e., $SoC_{i,t}^{\mathrm{B,av}} \pm SoC_{i,t}^{\mathrm{DB}}/2$). Finally, the total response intensity and discomfort are combined as a convex combination with parameterλ.

The comparison of the physical, DIUs, DDUs, and comfortable SoC bounds ($\overline{SoC}_{i,t}^{\mathrm{C}}$ and $\underline{SoC}_{i,t}^{\mathrm{C}}$) are shown in Fig.1. Since the focus herein is CCO, the uncertain SoC bounds are illustrated with rainbow color to represent the different probability levels. Remarks on DDU intuition, structure, probability distributions follow next:

Remark (Intuition on incentives and discomfort). During the expansion stage, the effects of the incentive outweighs the discomfort, however, discomfort levels are increasing. Thus, the mode of the upper available DDU bound, $\overline{SoC}_{i,t}^{\mathrm{DDU}}$, shifts from $g(\overline{SoC}_{i,t}^{\mathrm{DIU}}, c_{\mathrm{c},i,t}^{\mathrm{S}})$ to upper available DIU bound $\overline{SoC}_{i,t}^{\mathrm{DIU}}$. Similarly holds for the lower available DDU bound, $\underline{SoC}_{i,t}^{\mathrm{DDU}}$, and lower available DIU bound, $\underline{SoC}_{i,t}^{\mathrm{DIU}}$. During the contraction stage, when incentive effects are dominated by discomfort effects, discomfort levels are decreasing, i.e., the mode continues to decline from $\overline{SoC}_{i,t}^{\mathrm{DIU}}$ and $\underline{SoC}_{i,t}^{\mathrm{DIU}}$ to $\overline{SoC}_{i,t}^{\mathrm{C}}$ and $\underline{SoC}_{i,t}^{\mathrm{C}}$, respectively.

Remark (Structure). The functions g and h can be generalized via learning from test data. More generally, g could be an affine function based on price elasticity [4] and h can be a polynomial function. In Section V, we present a convex structure for DDUs.

Remark (Probability distributions). Function g and h are associated with probability distribution that can be determined by the Kolmogorov-Smirnov test from real-world actions. Specially, truncated normal distribution can be used to describe the expansion associated with incentive payment, and unimodal distribution can be used to describe the contraction associated with response discomfort.

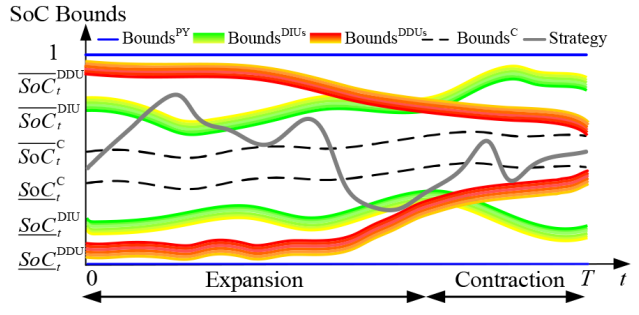

Fig. 1. Visualization of DIUs and DDUs in SoC bounds.

The scope of the uncertainties in the proposed ED problem are limited to the options presented above with DIU(a-c) and DDU(a-b). That is, other uncertainties, such as annualized capacity degradation, is deemed outside of scope and is not included in this paper. Next, we incorporate DIU(b-c) and DDU(a-b) into ED formulation, while DIU(a) is the focus of Section VI.

IV. Chance-constrained Optimization under DIUs and DDUs

A. Original Problem Formulation

In this paper, we consider DA-ED problem for a microgrid. The microgrid system operator aggregates GESs assets (e.g., TCL-GES and BES-GES), RES assets (e.g., wind and solar generation), and conventional loads. The goal of the system operator of the microgrid is to supply a DA dispatch of the assets to minimize operational costs while maintaining the power balance and considering various DIUs and DDUs. The full formulation is detailed next. First, consider the objective function:

$$\min_{\mathbf{y}} \; G(\boldsymbol{y},\boldsymbol{z}) = \sum_{t\in\boldsymbol{\Omega}_T} (C_t^{\mathrm{S}} + C_t^{\mathrm{G}}) \tag{6}$$

$$C_t^{\mathrm{S}} = \sum_{i\in\boldsymbol{\Omega}_G} (c_{\mathrm{d},i,t}^{S} P_{\mathrm{d},i,t} + c_{\mathrm{c},i,t}^{S} P_{\mathrm{c},i,t}) \Delta t \tag{7a}$$

$$C_t^{\mathrm{G}} = c_t^{\mathrm{G}} P_t^{\mathrm{G}} \Delta t. \tag{7b}$$

The operational cost includes the incentive cost of GESs C_t^{S} and the cost of power bought from the grid C_t^{G}. The power imported from the grid is denoted as P_t^{G}. DA time of use (ToU) price is given by c_t^{G}. The marginal costs of PV and WT assets are zero. Set of random parameters described in Section III is given by $\boldsymbol{z}$, set of decision variables is given by $\boldsymbol{y} := \{P_{\mathrm{d},i,t}, P_{\mathrm{c},i,t}, P_t^{\mathrm{G}}, SoC_{i,t}, RD_{i,t}\}$. Next, we will present the constraints of the ED optimization formulation.

GES chance constraints: $\forall t \in \boldsymbol{\Omega}_T$, $\forall i \in \boldsymbol{\Omega}_G$

$$\mathsf{P}(P_{\mathrm{c},i,t} \leq \overline{P}_{\mathrm{c},i,t}) \geq 1-\gamma \tag{8a}$$

$$\mathsf{P}(P_{\mathrm{d},i,t} \leq \overline{P}_{\mathrm{d},i,t}) \geq 1-\gamma \tag{8b}$$

$$\mathsf{P}(\underline{SoC}_{i,t} \leq SoC_{i,t}) \geq 1-\gamma \tag{8c}$$

$$\mathsf{P}(SoC_{i,t} \leq \overline{SoC}_{i,t}) \geq 1-\gamma, \tag{8d}$$

Where $1-\gamma$ ensures a probability of violation smaller than γ.

Chance constrained power balance: $\forall t \in \boldsymbol{\Omega}_T$

$$\mathsf{P}\left(\sum_{i\in\boldsymbol{\Omega}_R} P_{i,t}^{\mathrm{R}} + \sum_{i\in\boldsymbol{\Omega}_S} (P_{\mathrm{d},i,t} - P_{\mathrm{c},i,t}) + P_t^{\mathrm{G}} \geq P_t^{\mathrm{L}}\right) \geq 1-\gamma, \tag{9}$$

where $P_{i,t}^{\mathrm{R}}$ and P_t^{L} are the stochastic RES and load powers, while RES includes wind and solar generation from RES set $\boldsymbol{\Omega}_R$.

Other constraint: $\forall t \in \boldsymbol{\Omega}_T$

$$0 \leq P_t^{\mathrm{G}} \leq \overline{P}^{\mathrm{G}}, \tag{10}$$

where $\overline{P}^{\mathrm{G}}$ is the maximum power import from the grid. Next, we present the complete DIU and DDU formulations.

Complete CCO-DIUs & CCO-DDUs formulations:

The overall problem with DIUs and DDUs can be formulated as:

$$\begin{aligned} \min_{\boldsymbol{y}} \; & G(\boldsymbol{y},\boldsymbol{z}) \\ \text{s.t.} \; & \text{(1a-1f), (8a-8d), (9-10), (CCO-DIUs)} \\ & \text{(5a-5c) (CCO-DDUs)} \end{aligned} \tag{11}$$

The difference mainly lies in the consideration of DDUs (5a) - (5c)), besides traditionally considered DIUs. The CCO-DIU is a convex optimization formulation, however, the CCO-DDU is only guaranteed to be convex for specific structure of DDUs and certain conditions. This proof is developed in Appendix A.

B. Problem Reformulation

(a) Chance-constrained reformulation under DIUs:

Without using scenario-based methods, chance constraints (8a)-(8d), (9) admit a deterministic and tractable reformulation. We employ the standard reformulation from [11], and yields:

$$P_{\mathrm{c},i,t} \le \mu_{\overline{P}_{\mathrm{c},i,t}} - F^{-1}_{\overline{P}_{\mathrm{c},i,t}}(1-\gamma)\sigma_{\overline{P}_{\mathrm{c},i,t}} \tag{12a}$$

$$P_{\mathrm{d},i,t} \le \mu_{\overline{P}_{\mathrm{d},i,t}} - F^{-1}_{\overline{P}_{\mathrm{d},i,t}}(1-\gamma)\sigma_{\overline{P}_{\mathrm{d},i,t}} \tag{12b}$$

$$SoC_{i,t} \le \mu_{\overline{SoC}_{i,t}} - F^{-1}_{\overline{SoC}_{i,t}}(1-\gamma)\sigma_{\overline{SoC}_{i,t}} \tag{12c}$$

$$SoC_{i,t} \ge \mu_{\underline{SoC}_{i,t}} + F^{-1}_{\underline{SoC}_{i,t}}(1-\gamma)\sigma_{\underline{SoC}_{i,t}} \tag{12d}$$

$$\sum_{i\in\Omega_R}(\mu_{P^{\mathrm{R}}_{i,t}} - F^{-1}_{P^{\mathrm{R}}_{i,t}}(1-\gamma)\sigma_{P^{\mathrm{R}}_{i,t}}) + P^{\mathrm{G}}_t + \sum_{i\in\Omega_S}(P_{\mathrm{d},i,t} - P_{\mathrm{c},i,t}) \ge \mu_{P^{\mathrm{L}}_t} + F^{-1}_{P^{\mathrm{L}}_t}(1-\gamma)\sigma_{P^{\mathrm{L}}_t} \tag{12e}$$

Where normalized inverse cumulative distribution function F^{-1} can be obtained by Monte Carlo sampling (MCS) [27] of any kind of distribution (e.g., normal distribution, beta distribution).

(b) Chance-constrained reformulation under DDUs:

(R1) Robust Approximation: For reformulation under DDUs, the value of $F^{-1}(1-\gamma, \boldsymbol{y})$ is unknown before optimization. Thus, generalizations of the Cantelli's inequality can be used to estimate the best probability bound (i.e., the maximum value of $F^{-1}(1-\gamma,\boldsymbol{y})$) according to different general information about the distribution, with both mean and variance. The maximum values of $F^{-1}(1-\gamma,\boldsymbol{y})$ for six widely used distributions are derived and listed in Table II and these can be readily employed in any CCO-DDUs problems without complete knowledge of DDUs distribution. The supporting proofs are provided in Appendix B. The value is decreased with increasing security levels. Besides, the upper listed in Table II are with less available information of distribution but with higher and more robust value, which will further lead to higher security levels and tighter bounds. Since we do not know the exact distribution of DDUs in advance, but at least we can obtain the approximate shape of the distribution (e.g., unimodal or symmetric, etc.) through some live measurements or prior knowledge. For instance, if the unknown distribution is a Beta-like distribution, the unimodal function (Type 3) can be used to yield a robust reformulation that is less conservative than types 1 and 2. Robust approximation can guarantee a more conservative but credible solution to CCO-DDUs, which is specialized for high-security requirement and initial state of operations without sufficient historical data. To optimize with specific g,h distributions for DDUs, we next present an iterative algorithm.

(R2) Iterative Algorithm: We propose an iterative algorithm in Algorithm 1 for more precise structure (known function and distribution of *g* and *h*), if sufficient live measurement/data about GES are provided. Robust reformulation (R1) is used as starting point of $F^{-1}(1-\gamma,\boldsymbol{y}_k)$ and it will be updated with updated strategy $\boldsymbol{y}_{k-1}$ via MCS. The convergence of the iterative algorithm is determined by the convexity of CCO-DDUs, also shown in Appendix A.

TABLE II
APPROXIMATION OF WIDELY USED NORMALIZED INVERSE CUMULATIVE DISTRIBUTION

Type & Shape	$F^{-1}(1\quad\gamma,\boldsymbol{y})_{\max}$	γ
1) No distribution assumption	$\sqrt{(1\quad\gamma)/\gamma}$	$0<\gamma\quad 1$
2) Symmetric distribution	$\sqrt{1/2\gamma}$	$0<\gamma\quad 1/2$
	0	$1/2<\gamma\quad 1$
3) Unimodal distribution	$\sqrt{(4\quad 9\gamma)/9\gamma}$	$0<\gamma\quad 1/6$
	$\sqrt{(3\quad 3\gamma)/(1+3\gamma)}$	$1/6<\gamma\quad 1$
4) Symmetric & unimodal distribution	$\sqrt{2/9\gamma}$	$0<\gamma\quad 1/6$
	$p\frac{}{3}(1\quad 2\gamma)$	$1/6<\gamma\quad 1/2$
	0	$1/2<\gamma\quad 1$
5) Student's *t* distribution	$t^{-1}_{\nu,\sigma}(1\quad\gamma)$	$0<\gamma\quad 1$
6) Normal distribution	$\Phi^{-1}(1\quad\gamma)$	$0<\gamma\quad 1$

Algorithm 1 Iterative algorithm for CCO-DDUs

Input: Probability level γ, convergence criterion δ, deterministic and reformulated random parameters under DIUs.
Output: Decision variables $\boldsymbol{y}$ and cost function $F(\boldsymbol{y},\boldsymbol{z})$.
Step 1 - Initialization:
Set $k=0$, and $F^{-1}(1-\gamma,\boldsymbol{y}_0)$ with robust reformulation value referred to Table II. Compute CCO-DDUs with $F^{-1}(1-\gamma,\boldsymbol{y}_0)$ to obtain initial value of $\boldsymbol{y}_0$. Use $\boldsymbol{y}_0$ to update $F^{-1}(1-\gamma,\boldsymbol{y}_1)$ via MCS. Calculate $\epsilon_k = \left|F^{-1}(1-\gamma,\boldsymbol{y}_1) - F^{-1}(1-\gamma,\boldsymbol{y}_0)\right|$.
Step 2 - Iteration:
While $\epsilon_k > \delta$ **do**
  $k \leftarrow k+1$
  Compute CCO-DDUs with $F^{-1}(1-\gamma,\boldsymbol{y}_k)$ to obtain $\boldsymbol{y}_k$.
  Use $\boldsymbol{y}_k$ to update $F^{-1}(1-\gamma,\boldsymbol{y}_{k+1})$ via MCS.
  Calculate $\epsilon_k = \left|F^{-1}(1-\gamma,\boldsymbol{y}_{k+1}) - F^{-1}(1-\gamma,\boldsymbol{y}_k)\right|$.
end
Step 3 - Return: $\boldsymbol{y}=\boldsymbol{y}_k$, $G(\boldsymbol{y},\boldsymbol{z})=G(\boldsymbol{y}_k,\boldsymbol{z})$

V. NUMERICAL ANALYSIS

The system is set up with ground truth data obtained from the Pecan Street dataset and used for the data-driven analysis of 100 TCL units as GES units. Historical data of RES u nit and demand are collected from the urban distribution area of Jiangsu province, China in 2020. The tiered electricity price of Jiangsu province, China, is used for day-ahead electricity price. All the data used in this paper are publically available [26]. Optimization problems are coded in MATLAB with YALMIP interface and solved by GUROBI 9.5 solver. The programming environment is Core i7-1165G7 @ 2.80GHz laptop with 16GB RAM.

A. Baseline Results Compared with Different Models

We next compute and compare the solutions of three test models (M1-M3) that differ in how they incorporate uncertainty in the optimization formulation:

(M1) Deterministic LP: this deterministic baseline model of GES was proposed in [9] and considers no uncertainties and no time-varying parameters (i.e., assumes large SoC bounds and averaged exogenous conditions), rendering an LP with constant parameters.

(M2) CCO-DIUs: this stochastic baseline model uses CCO with DIUs, which is common in the literature [11], [15], and yields a decision-independent CCO problem with varying, stochastic SoC bounds.

(M3) CCO-DDUs: this CCO model illustrates the novel convex DDU structure along with different DIUs. The formulation then reflects a decision-dependent CCO problem.

We first adopt a linear structure, as shown in (13) below,

$$g=\begin{cases}(\overline{SoC}_{i,t}^{\mathrm{PY}}-\overline{SoC}_{i,t}^{\mathrm{DIU}})\mathcal{N}(\mu_{g^{\mathrm{U}}},\sigma_g)+\overline{SoC}_{i,t}^{\mathrm{DIU}}\\(\underline{SoC}_{i,t}^{\mathrm{PY}}-\underline{SoC}_{i,t}^{\mathrm{DIU}})\mathcal{N}(\mu_{g^{\mathrm{L}}},\sigma_g)+\underline{SoC}_{i,t}^{\mathrm{DIU}}\end{cases} \tag{13a}$$

$$h=\begin{cases}(\overline{SoC}_{i,t}^{\mathrm{C}}-Q_{g^{\mathrm{U}}})\mathcal{LN}(\mu_{h^{\mathrm{U}}},\sigma_h)+Q_{g^{\mathrm{U}}}\\(\underline{SoC}_{i,t}^{\mathrm{C}}-Q_{g^{\mathrm{L}}})\mathcal{LN}(\mu_{h^{\mathrm{L}}},\sigma_h)+Q_{g^{\mathrm{L}}}\end{cases} \tag{13b}$$

$$\mu_{g^{\mathrm{U/L}}}=c_{\mathrm{c/d},i,t}^{\mathrm{S}}/\bar{c}^{\mathrm{S}},\ \mu_{h^{\mathrm{U/L}}}=\beta_i^{\mathrm{U/L}}RD_{i,t}, \tag{13c}$$

Where normal distribution g and lognormal distribution h describe the DDUs. The quantile function of g is defined as Q_g. We set $\bar{c}^{\mathrm{S}}=1.5$, $c_{\mathrm{c},i,t}^{\mathrm{S}}$=0.3, $c_{\mathrm{d},i,t}^{\mathrm{S}}$=0.6, $\beta_i^{\mathrm{U}}=3$, $\beta_i^{\mathrm{L}}=6$, $\sigma_g=0.5$, $\sigma_h=0.1$, λ=0.7. The different sets of prices and discomfort aversion factors beget trade-off between charging and discharging actions. The ToU pricing is set to be 0.5-0.9-1.4 (CNY/kWh) while the security level for CCO is set to be 95%.

Comparisons of M1-M3 are shown in Fig. 2 while Table III summarizes the results. Great difference has been observed between M1-M3 concerning the SoC distribution and charge/discharge power. GES units discharge for most of the time and maintain the lowest SoC during peak load in M1, while the discharge response is reduced evidently after 16 h in M2 & M3 to guarantee the available lower SoC bound, which results in a charging action at the end of dispatch. In terms of optimality, M3 operations represent the highest costs, because a trade-off is exacted between comfort and revenue. The other optimization results mainly focus on the difference in SoC bounds shown in Fig. 3 (a). It is observed that SoC bounds are reduced in M2 because of compressed temperature preference (i.e., customers' behavior), while SoC is limited within [0,1] in M1 and significantly over-estimate the capability of GES. Additionally, the difference between SoC bounds are shown in Fig. 3(b). Compared with DIU bounds, the expansion effect is witnessed in M3 before 11 am and then followed with contraction effects. And the average expansion and contraction percentage for (Upper and lower) bounds are ([8.6,37.0]%,[-5.9,-42.0]%). It's observed that the accumulated discharging actions increase the discomfort and reduce the expansion effect in the morning, then the increased contraction effect mainly results from the SoC-based discomfort in the afternoon. The recovery of SoC to the comfortable bounds causes the reduced contraction effect in the evening. But the deviation from comfortable bounds increases contraction effect at night peak load period.

TABLE III
OPTIMIZATION RESULTS WITH DIFFERENT MODELS AND UNCERTAINTIES

Metric	M1	M2	M3
$\mathrm{Cost}^{\mathrm{OC}}$ (CNY)	2034.6	2727.6	2799.7
$\sum P_{\mathrm{d},i,t}\Delta t$ (kWh)	750.6	337.9	164.9
$\sum P_{\mathrm{c},i,t}\Delta t$ (kWh)	35.7	60.5	40.3
$\sum P_t^{\mathrm{G}}\Delta t$ (kWh)	1495.1	2288.8	2443.2

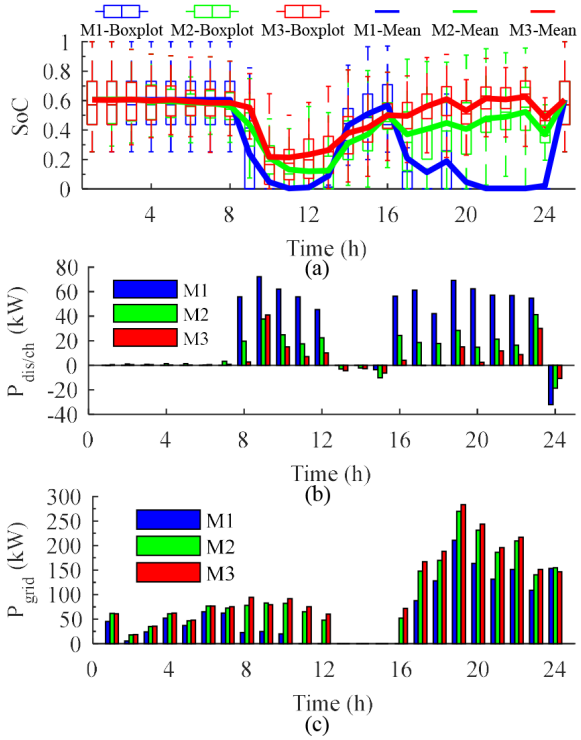

Fig. 2. Comparison between model (1) & (2): (a) SoC distribution, boxplot: distribution of individual GES units, thick line: mean value of GES portfolio, (b) aggregated charge or discharge power, (c) power from grid.

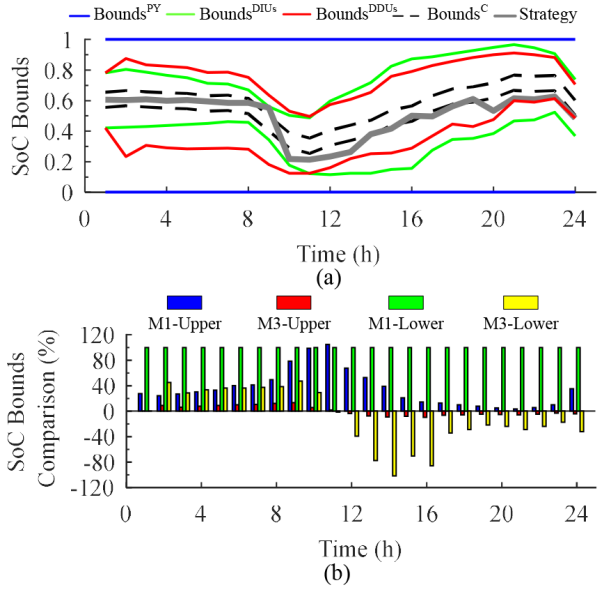

Fig. 3. (a) Comparison between different SoC bounds, (b) expansion or contraction effect compared with DIU bounds

Moreover, it is observed that SoC changes are not consistent with grid response because different power actions exist (e.g., grid net charge, energy losses from self discharge, additional energy input from baseline consumption). Different power actions of M3 are illustrated in Fig. 4, where self discharge changes with SoC and is always negative. Additional energy input is always positive and calculated based on baseline SoC. And it is clear that the residual flexibility

and capacity for grid response is quite limited compared with other energy actions, which has been overlooked in prior work [9].

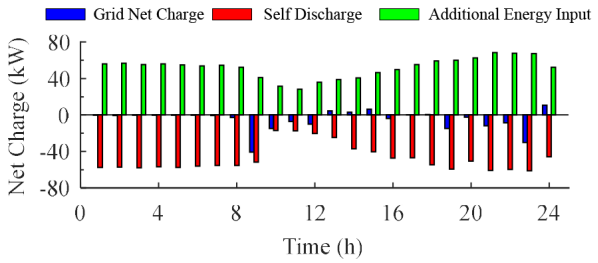

Fig. 4. Comparison between different parts of power actions of M3.

B. Benefit from considering DDUs

At first glance, the results of M1 and M2 appear superior to M3. This is due to M1 and M2 having greedy utilization of flexibility and low operational costs. However, the predicted results of M1 and M2 are unlikely to be realized in practice due to a lack of reliability of dispatch and the unavailability of GES units [10], [24]. To capture these practical shortcomings of M1 and M2, we introduce two reliability indices in this paper to assess the difference between predicted strategies and real actions: i) loss of response power probability (*LORP*) and ii) expected response energy not served (*ERNS*). The basic idea is to compare the difference between practical SoC bounds (calculated with DDUs effect) and predicted SoC bounds from the different models. The indices are defined in (14), where $X_k|\boldsymbol{y},\boldsymbol{z}$ represents the reliability loss events under strategy $\boldsymbol{y}$ and uncertainty $\boldsymbol{z}$. $R(.|.)$ is the function of response energy losses and can be calculated by the deviation of SoC strategy from the practical SoC bounds.

$$LORP = \sum_k \mathsf{P}(X_k|\boldsymbol{y},\boldsymbol{z}) \tag{14a}$$

$$ERNS = \sum_k \mathsf{P}(X_k|\boldsymbol{y},\boldsymbol{z}) R(X_k|\boldsymbol{y},\boldsymbol{z}). \tag{14b}$$

Fig. 5 shows the reliability performance comparison between M1-M3 with respect to SoC bounds and reliability indices. Practical SoC bounds are illustrated by gradient colors to represent uncertain bounds with different probability level (darker for higher probability level). Compared with theoretical SoC bounds, the practical ones contracted gradually in M1-M2 and end with few flexibility to response. This provides a convincing explanation of the response unavailability of DR, especially during the peak load period using previous greedy strategies. While theoretical bounds are a little more conservative than practical ones in M3 using robust approximation method. In terms of reliability indices, lower reliability (i.e., higher LORP & ERNS) are revealed in M1-M2 due to the overestimation of the feasible region. The negative value of ERNS represents the under-response of GES units during the expansion stage, while the positive one represents the over-response of GES units during the contraction stage. Moreover, the expected reliability results shown in Table IV indicate that the reliability indices are constant for M1 regardless of the security level, while the reliability performance of M2 and M3 worsen for operations with a lower security level. And the reliability indices using M1/M2 are far beyond the security level $1-\gamma$, while results of M3 are maintained within the security level. In practice, decision-makers would determine γ according to their risk preference, which is a trade-off between costs and risks. Additionally, the penalty cost (PC) and total cost (TC) are compared under 0.8 times of ToU price for over-response and 1.5 times of ToU price for under-response. The higher (actual) penalty and total cost from M1/M2 are compared with the theoretical operational costs (OC) listed in Table IV. Clearly, the improved reliability and overall economic performance illustrates how optimization under DDUs can provide an admissible strategy, improve the availability of delivery of grid services and reduce the penalty cost.

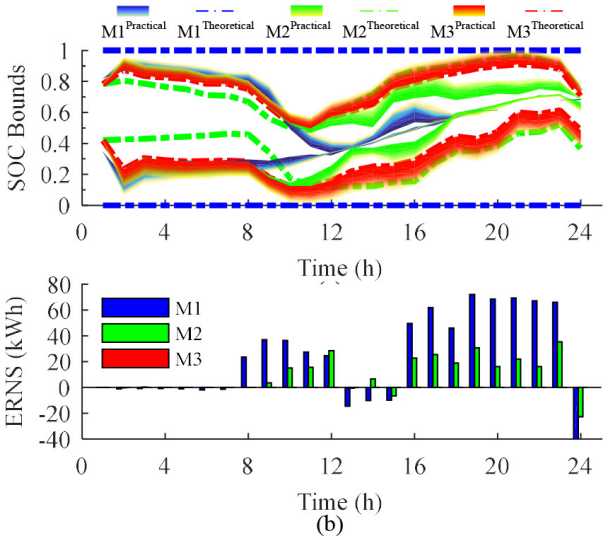

Fig. 5. Reliability performance comparison with respect to (a) practical and theoretical SoC bounds (95%) and (b) ERNS.

TABLE IV
RELIABILITY AND ECONOMIC PERFORMANCE OF DIFFERENT MODELS AND PROBABILITY LEVEL

γ	Indices	M1	M2	M3
0.05	*LORP* / *ERNS*		0.3 / 12.0	0.0 / 0.0
	Cost^{PC} / Cost^{TC}	*LORP* 0.6	429.2 / 3156.8	0.0 / 2799.7
0.25	*LORP* / *ERNS*	*ERNS* 30.6	0.4 / 14.0	0.1 / 3.0
	Cost^{PC} / Cost^{TC}	Cost^{PC} 1246.7	517.3 / 3244.9	0.0 / 2799.7
0.45	*LORP* / *ERNS*	Cost^{TC} 3281.3	0.4 / 15.2	0.2 / 3.6
	Cost^{PC} / Cost^{TC}		573.2 / 3300.8	0.0 / 2799.7

C. Flexibility with Different Dispatch Modes and DDUs Structure

The increasing contraction effect on SoC bounds shown in Fig. 3 indicates that it is not suitable for the system operator to fully leverage the flexibility of GES units throughout the day, but it may be better to use GES for short-time period to reduce the contraction effect. Thus, in this subsection, we consider additional dispatch modes: (D1) all-day dispatch, and (D2) peak-time dispatch (7 pm-10 pm). In addition, different RD structures are investigated for different GESs types. For example, BES owners wish to maximize unit lifetime, which emphasizes the disutility function (F1), while TCL and EV units employ both the disutility and SoC-based discomfort. TCL units may have symmetric levels of SoC-based discomfort, which can be modeled with absolute value or dead-band

function (F2). However, EV units just need to meet a minimum SoC threshold and discomfort can, thus, be modelled linearly (F3).

Herein, we only change the dispatch time duration and discomfort function while the other factors remain unchanged from the baseline case study. The comparison of flexibility and DDUs expansion/contraction effects are shown in Table V. Specifically, deviated from the SoC bounds under DIUs, the average expansion (EP) and contraction (CT) of the upper and lower SoC bounds are denoted as $\overline{\text{EP}}$, $\overline{\text{CT}}$ and $\underline{\text{EP}}$, $\underline{\text{CT}}$, respectively. It is observed that BES units outperform other GES units in terms of flexibility and cost due to BES units being relatively unaffected by DDUs. And the symmetrical effect of SoC-based discomfort inherently limits the flexibility utilization of TCL units and makes TCL units least economic in dispatch. More importantly, for typical days with night peak time, discharge quantity and contraction effect are two decisive factors, while charge actions and expansion effect are not relatively important because they rarely contribute to the dispatch. And operations with more discharge actions (e.g., operations in F1) and less contraction effect (e.g., operations in D2) tend to perform more optimized. Finally, GESs with asymmetric DDUs structure and short-time period dispatch are more suggested to improve the DR performance.

TABLE V
OPERATIONS WITH DISPATCH MODES AND DDUS STRUCTURE

DDUs Structure	Dispatch Mode	Cost^{TC} (CNY)	$\sum P_{\text{d},i,t}\Delta t$ (kWh)	$\sum P_{\text{c},i,t}\Delta t$ (kWh)	$\overline{\text{EP}}$ (%)	$\underline{\text{EP}}$ (%)	$\overline{\text{CT}}$ (%)	$\underline{\text{CT}}$ (%)
F1	D1	2772.4	187.8	31.7	9.4	37.9	-4.2	-26.7
	D2	2749.2	174.3	0.8	0.0	7.5	-0.4	-0.7
F2	D1	2799.7	164.9	40.3	8.6	37.0	-5.9	-42.0
	D2	2766.5	152.7	0.9	2.6	28.8	-3.1	-13.3
F3	D1	2785.4	171.2	32.1	9.4	39.8	-4.8	-31.2
	D2	2755.8	167.1	1.4	0.2	13.2	-1.8	-5.4

D. Computational performance of the convex reformulation

In this subsection, the convergence of reformulated methods to optimality is shown in Fig. 6 with two common types of distributions (Beta and Lognormal) applied to h. It can be seen that the iterative algorithm converges within 4 iterations. Moreover, the optimization results compared with two reformulated methods are shown in Table VI, where both distributions adopt the robust value of the unimodal type. The solution time depends on the complexity of function of response discomfort and distribution of DDUs (more time for Beta distribution and absolute function of TCL). And it is obvious that R1 outperforms R2 in terms of computational efficiency, but it will produce more conservative results, while R2 achieves a lower cost. The optimality gap between two methods is within 1% which indicates that R1 can be used extensively even if the distribution of DDUs is unknown. Note that to improve the computational efficiency of the two reformulation methods, one can consider the following approaches: (i) employ a quadratic or polynomial approximation of the absolute function, which makes it more; (ii) reduce the number of DDU constraints by replacing the DDUs constraints of each individual GES unit with that of the entire GES portfolio; and (iii) reduce the convergence criterion for the iterative algorithms, which may not affect optimality gap significantly as shown in Fig. 6 achieving near-optimal performance after just 2 (two) iterations.

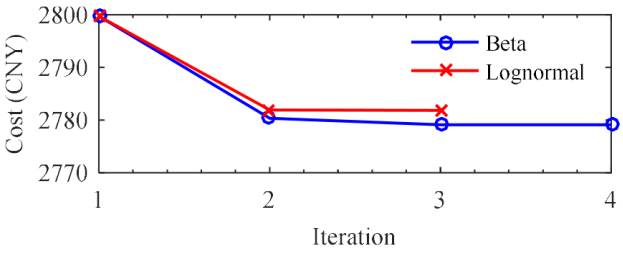

Fig. 6. Convergence performance under Beta and Lognormal distribution (95%)

TABLE VI
OPERATIONS COMPARED WITH DIFFERENT REFORMULATION METHODS

DDUs Structure	Distribution Type	R1		R2	
		Cost^{TC} (CNY)	Time (s)	Cost^{TC} (CNY)	Time (s)
F1	Beta Distribution	2772.4	24.6	2750.0	2751.0
F2		2799.7	310.9	2779.1	6406.7
F3		2785.4	28.0	2764.3	3032.2
F1	Lognormal Distribution	2772.4	24.6	2752.3	132.1
F2		2799.7	310.9	2781.9	1562.9
F3		2785.4	28.0	2766.6	103.9

Finally, sensitivity analysis is performed to compare the optimality gap with different standard deviations and probability level of DDUs (only for the Lognormal distribution). The results shown in Fig. 7 indicates that the sensitivity of gap errors will decline at first and then increase when decreasing the security level. Moreover, it is found that that the relationship between optimality gap and the distributions' standard deviation is almost linear, which helps decision-makers map levels to optimality.

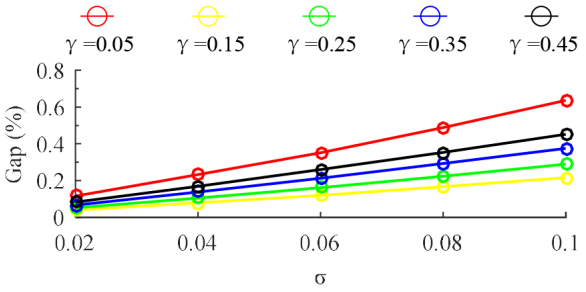

Fig. 7. Sensitivity of gap with probability level and standard deviations

VI. DISCUSSION OF EXTENDED PROBLEMS

Compared with deterministic ES, the key challenges to overcome for broad adoption of stochastic GES in power system operations include: (1) non-trivial energy losses due to self-discharge and uncertain baseline consumption; (2) time-varying parameters and flexibility; (3) DIUs and DDUs in SoC bounds; (4) on-off state probability due to customers' behavior. The prior case studies accurately mitigates effects of challenges (1-3), so in this subsection, we further propose two approaches to mitigate challenge (4).

(S1) - Portfolio with Deterministic Reserve

The on-state probability tends to be quite low especially for night-time and working hours in the residential sector, so system

operators could participate in DA reserve market to enhance the security level under the support of deterministic reserve, such as ES and CPP. For those units below the security level, deterministic reserves will replace the unavailable response of GES as $P^{\mathrm{RS}}_{i,t}$, and the constraints for deterministic reserves are added as (15):

$$\underline{P}^{\mathrm{RS}}_{i,t} \le P^{\mathrm{RS}}_{i,t} \le \overline{P}^{\mathrm{RS}}_{i,t} \tag{15a}$$

$$-P^{\mathrm{RS}}_{i,\mathrm{RD}} \le P^{\mathrm{RS}}_{i,t+1} - P^{\mathrm{RS}}_{i,t} \le P^{\mathrm{RS}}_{i,\mathrm{RU}} \tag{15b}$$

$$P^{\mathrm{RS}}_{i,t} = P_{\mathrm{d},i,t} - P_{\mathrm{c},i,t}, \tag{15c}$$

where upper and lower power reserve bounds are denoted $\underline{P}^{\mathrm{RS}}_{i,t}$ and $\overline{P}^{\mathrm{RS}}_{i,t}$, respectively. The ramp rates are given by $P^{\mathrm{RS}}_{i,\mathrm{RD}}$ and $P^{\mathrm{RS}}_{i,\mathrm{RU}}$.

(S2) - Portfolio with Probabilistic Reserve

It can be costly to use 100% reliable reserve for normal grid operations, so here we explore probabilistic reserves as an alternative [28]. The reliability requirement of combined probabilistic reserve, and its cost are shown in (16), where $R^{\mathrm{RS}}_{i,t}$ is the reliability of probabilistic reserve and $c^{\mathrm{RS}}_{i,t}$ is the corresponding price:

$$(1-p_{i,t})(1-R^{\mathrm{RS}}_{i,t}) = \gamma, \quad c^{\mathrm{RS}}_{i,t} = a^{\mathrm{RS}} (R^{\mathrm{RS}}_{i,t})^{b^{\mathrm{RS}}}. \tag{16}$$

First, the on-state probability of 100 TCL-GESs is analyzed and the maximum and minimum average on-state probability are 0.99 and 0.83, respectively. The corresponding time periods are 7 pm and 9 am, respectively. Thus, the real-time security level for DR produced by TCL-GES units can be described as $p_{i,t}(1-\gamma)$, so system operators should rely on other reserves to guarantee the system security requirement $(1-\gamma)$. For reserve price, we set $a^{\mathrm{RS}} = 1$ (100% reliability), $b^{\mathrm{RS}} = 2$, and we compute the modified results with different solution methods. Results for S1 and S2 shown in Table VII are more credible but less economic than just considering challenges (1-3). It is observed that the power demand of GESs is reduced and transferred to demand of reserve instead, and the demand of reserve is gradually reduced with the decrease of security level. Moreover, portfolio with probabilistic reserves outperforms the deterministic ones in terms of overall cost.

TABLE VII
MODIFIED RESULTS WITH TWO TYPES OF RESERVE

	S1			S2		
γ	$\mathrm{Cost}^{\mathrm{TC}}$ (CNY)	$\sum P_{\mathrm{c/d},i,t}\Delta t$ (kWh)	$\sum P^{\mathrm{RS}}_{i,t}\Delta t$ (kWh)	$\mathrm{Cost}^{\mathrm{TC}}$ (CNY)	$\sum P_{\mathrm{c/d},i,t}\Delta t$ (kWh)	$\sum P^{\mathrm{RS}}_{i,t}\Delta t$ (kWh)
0.05	2835.4	63.8	119.1	2839.3	51.0	121.0
0.30	2519.2	25.4	190.6	2511.4	37.3	184.9
0.55	2351.8	10.3	216.7	2347.2	15.4	213.9
0.80	2174.0	0.00	232.2	2174.0	0.0	232.2

VII. CONCLUSION

In this paper, we proposed a novel CCO formulation for the day-ahead economic dispatch of uncertain GES units, which fully incorporates dynamic properties and various types of DIUs and DDUs. Specially, we modelled the human behavior of GES units as the endogenous uncertain SoC bounds affected by incentive signals and discomfort levels. The numerical results show that the dynamic flexibility of GES units is reduced and limited by DDUs effect and time-varying user preferences. And by considering DDUs, we enable decision-makers to systematically trade-off between overall profit and customers' (dis)comfort ranges. This produces more conservative, but more credible strategies. These results illustrate how improved availability and economic performance of uncertain GES units can benefit practical DR programs. In addition, we proposed two tractable solution methods for CCO-DDUs while the computational performance shows that a robust approximation outperforms the iteration algorithm in computational efficiency (by a few minutes) while maintaining a good performance (within 1% optimality gap). And the major attraction is that robust approximation can be applicable in any CCO problem without complete knowledge of DDUs, which is more applicable to be used as the black start of DR programs.

Future work will focus on reducing the risk of GES units and achieving a trade-off between expected profit and risk by considering investment portfolio optimization in multiple markets. In addition, measurements/data from GES units should be further analyzed to possibly infer and learn the structure of DDUs.

APPENDIX

A. Convexity and Convergence Conditions

According to the convexity condition of CCO and reformulation (13c-13d), CCO-DDUs problem (11) is only guaranteed to be convex under the condition (i)-(ii). The convergence of the iterative algorithm is guaranteed when the convexity condition is satisfied [29].

(i) $\mu_{\underline{SoC}_{i,t}}$ and $F^{-1}_{\underline{SoC}_{i,t}}(1-\gamma)\sigma_{\underline{SoC}_{i,t}}$ are convex function of decision variables $\boldsymbol{y}$.

(ii) $-\mu_{\overline{SoC}_{i,t}}$ and $F^{-1}_{\overline{SoC}_{i,t}}(1-\gamma)\sigma_{\overline{SoC}_{i,t}}$ are convex function of decision variables $\boldsymbol{y}$.

For DDUs designed in (13), the inside functions are given:

$$\mu_{\overline{SoC}_{i,t}} = (\overline{SoC}^{\mathrm{B}}_{i,t} - Q_{g^{\mathrm{U}}})\beta^{\mathrm{U}}_i RD_{i,t} + Q_{g^{\mathrm{U}}} \tag{17a}$$

$$\mu_{\underline{SoC}_{i,t}} = (\underline{SoC}^{\mathrm{B}}_{i,t} - Q_{g^{\mathrm{D}}})\beta^{\mathrm{D}}_i RD_{i,t} + Q_{g^{\mathrm{D}}} \tag{17b}$$

$$F^{-1}_{\overline{SoC}_{i,t}}(1-\gamma)\sigma_{\overline{SoC}_{i,t}} = (Q_{g^{\mathrm{U}}} - \overline{SoC}^{\mathrm{B}}_{i,t})F^{-1}_{h^{\mathrm{U}}}(1-\gamma,\boldsymbol{y})\sigma_{h^{\mathrm{U}}} \tag{17c}$$

$$F^{-1}_{\underline{SoC}_{i,t}}(1-\gamma)\sigma_{\underline{SoC}_{i,t}} = (Q_{g^{\mathrm{D}}} - \underline{SoC}^{\mathrm{B}}_{i,t})F^{-1}_{h^{\mathrm{D}}}(1-\gamma,\boldsymbol{y})\sigma_{h^{\mathrm{D}}} \tag{17d}$$

Thus, the convexity conditions are further simplified as:
(a) $RD_{i,t}$ is a convex function of $\boldsymbol{y}$.
(b) $F^{-1}_h(1-\gamma,\boldsymbol{y})$ is a convex function of $\boldsymbol{y}$.

The convex function described in (5c) guarantees the convexity condition (a). And since we fix the variance of the distribution, the convexity of $F^{-1}_h(1-\gamma,\boldsymbol{y})$ is equivalent to the convexity of $F^{-1}_h(1-\gamma,\mu)$. For lognormal distributions, $F^{-1}_h(1-\gamma,\mu) = \exp(\mu + \sqrt{2\sigma^2}\mathrm{erf}^{-1}(1-2\gamma))$, which guarantees the convexity condition (b). While, for other complex distributions (e.g., Beta), there is no explicit expression for the inverse CDF, and numerical simulations in Fig. 8 shows that it can not guarantee convexity overall. There exists, however, a convex region which contains the iterations using Beta distribution. Thus, global optimality can be verified for this convex region and corresponding constraints can be added to limit response discomfort (μ) of GES units within that region.

B. Proof of the value of Robust Approximation

We write F the CDF function, P the PDF function, $k \ge 0$ a constant, and ξ as the probabilistic parameter with zero mean and unit variance under the chosen distribution. Different versions of Cantelli's inequality [30] are used to obtain the following results.

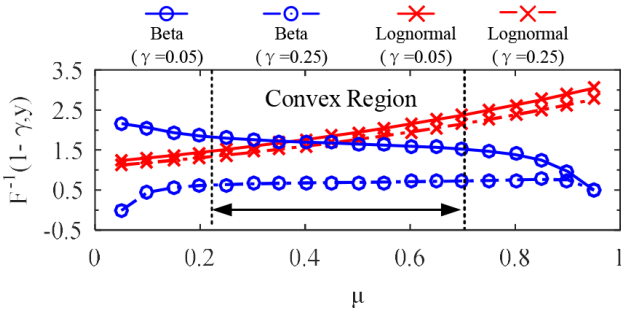

Fig. 8. Numerical test of convexity

1) Classical Cantelli inequality can be used without distribution assumption of DDUs and infers the following conclusion.

$$F(k)=1-\sup_{P\in NA}\mathsf{P}[\xi\geq k]=k^2/1+k^2 \tag{18a}$$

$$F^{-1}(1-\gamma)=\sqrt{(1-\gamma)/\gamma} \tag{18b}$$

2) Chebyshev's inequality can be used with symmetric distribution of DDUs and infers the following conclusion.

$$F(k)=1-\sup_{P\in S}\mathsf{P}[\xi\geq k]=1-\frac{1}{2}\sup_{P\in S}\mathsf{P}[|\xi|\geq k]=1-\frac{1}{2k^2} \tag{19a}$$

$$F^{-1}(1-\gamma)=\sqrt{1/2\gamma} \tag{19b}$$

3) VySoChanskij–Petunin inequality can be used with unimodal distribution of DDUs and infers the following conclusion.

$$F(k)=1-\sup_{P\in U}\mathsf{P}[\xi\geq k]$$
$$=\begin{cases}1-4/(9k^2+9) & k\geq\sqrt{5/3}\\ 1-(3-k^2)/(3+3k^2) & 0\leq k\leq\sqrt{5/3}\end{cases} \tag{20a}$$

$$F^{-1}(1-\gamma)=\begin{cases}\sqrt{2/9\gamma} & 0<\gamma\leq 1/6\\ \sqrt{3}(1-2\gamma) & 1/6<\gamma\leq 1/2\end{cases} \tag{20b}$$

4) Gauss's inequality can be used for symmetric & unimodal distribution of DDUs and infers the following conclusion.

$$F(k)=1-\sup_{P\in SU}\mathsf{P}[\xi\geq k]=1-\frac{1}{2}\sup_{P\in U}\mathsf{P}[|\xi|\geq k]$$
$$=\begin{cases}1-2/9k^2 & k\geq 2/\sqrt{3}\\ 1/2+k/2\sqrt{3} & 0\leq k\leq 2/\sqrt{3}\end{cases} \tag{21a}$$

$$F^{-1}(1-\gamma)=\begin{cases}\sqrt{2/9\gamma} & 0<\gamma\leq 1/6\\ \sqrt{3}(1-2\gamma) & 1/6<\gamma\leq 1/2\end{cases} \tag{21b}$$

5-6) For student's t and normal distribution of DDUs, the normalized CDFs $t^{-1}_{\nu,\sigma}(1-\gamma)$ and $\Phi^{-1}(1-\gamma)$ can be used without introducing approximation errors.

REFERENCES

[1] N. Mararakanye and B. Bekker, "Renewable energy integration impacts within the context of generator type, penetration level and grid characteristics," *Renew. Sust. Energ. Rev.*, vol. 108, pp. 441–451, 2019.

[2] J. Xi, "China proposed the "2030" and "2060" double carbon goal at the 75th united nations general assembly." [Online]. Available: http://www.gov.cn/xinwen/2020-09/22/content_5546168.htm?gov.

[3] IEA, "Global energy review 2021." [Online]. Available: https://www.iea.org/reports/global-energy-review-2021.

[4] Z. Chen, L. Wu, and Y. Fu, "Real-time price-based demand response management for residential appliances via stochastic optimization and robust optimization," *IEEE Trans. on smart grid*, vol. 3, no. 4, pp. 1822–1831, 2012.

[5] H. Zhong, L. Xie, and Q. Xia, "Coupon incentive-based demand response: Theory and case study," *IEEE Trans. on Power Systems*, vol. 28, no. 2, pp. 1266–1276, 2012.

[6] H. Liang, J. Ma, and J. Lin, "Robust distribution system expansion planning incorporating thermostatically-controlled-load demand response resource," *IEEE Trans. on Smart Grid*, vol. 13, no. 1, pp. 302–313, 2021.

[7] A. Niromandfam, A. M. Pour, and E. Zarezadeh, "Virtual energy storage modeling based on electricity customers' behavior to maximize wind profit," *Journal of Energy Storage*, vol. 32, p. 101811, 2020.

[8] Y. Xia, Q. Xu, and et al., "Bilevel optimal configuration of generalized energy storage considering power consumption right transaction," *Int. J. Electr. Power Energy Syst.*, vol. 128, p. 106750, 2021.

[9] M. Song, C. Gao, and et al., "Thermal battery modeling of inverter air conditioning for demand response," *IEEE Trans. on Smart Grid*, vol. 9, no. 6, pp. 5522–5534, 2017.

[10] B. Zeng, X. Wei, and et al., "Hybrid probabilistic-possibilistic approach for capacity credit evaluation of demand response considering both exogenous and endogenous uncertainties," *Applied energy*, vol. 229, pp. 186–200, 2018.

[11] M. Vrakopoulou, B. Li, and J. L. Mathieu, "Chance constrained reserve scheduling using uncertain controllable loads part i: Formulation and scenario-based analysis," *IEEE Trans. on Smart Grid*, vol. 10, no. 2, pp. 1608–1617, 2017.

[12] J. Zhang and A. D. Domínguez-García, "Evaluation of demand response resource aggregation system capacity under uncertainty," *IEEE Trans. on Smart Grid*, vol. 9, no. 5, pp. 4577–4586, 2017.

[13] L. Cheng, Y. Wan, and et al., "Evaluating energy supply service reliability for commercial air conditioning loads from the distribution network aspect," *Applied Energy*, vol. 253, p. 113547, 2019.

[14] N. Qi, L. Cheng, and et al., "Smart meter data-driven evaluation of operational demand response potential of residential air conditioning loads," *Applied Energy*, vol. 279, p. 115708, 2020.

[15] M. Amini and M. Almassalkhi, "Optimal corrective dispatch of uncertain virtual energy storage systems," *IEEE Trans. on Smart Grid*, vol. 11, no. 5, pp. 4155–4166, 2020.

[16] M. B. Kane and K. Sharma, "Data-driven identification of occupant thermostat-behavior dynamics," *arXiv preprint arXiv:1912.06705*, 2019.

[17] R. M. Apap and I. E. Grossmann, "Models and computational strategies for multistage stochastic programming under endogenous and exogenous uncertainties," *Comput Chem Eng.*, vol. 103, pp. 233–274, 2017.

[18] Y. Zhan, Q. Zheng, and et al., "Generation expansion planning with large amounts of wind power via decision-dependent stochastic programming," *IEEE Trans. on Power Systems*, vol. 32, no. 4, pp. 3015–3026, 2016.

[19] N. H. Lappas and C. E. Gounaris, "Robust optimization for decision-making under endogenous uncertainty," *Comput Chem Eng.*, vol. 111, pp. 252–266, 2018.

[20] O. Nohadani and K. Sharma, "Optimization under decision-dependent uncertainty," *SIAM Journal on Optimization*, vol. 28, no. 2, pp. 1773–1795, 2018.

[21] Q. Zhang and W. Feng, "A unified framework for adjustable robust optimization with endogenous uncertainty," *AIChE Journal*, vol. 66, no. 12, p. e17047, 2020.

[22] Y. Zhang, F. Liu, and et al., "Robust scheduling of virtual power plant under exogenous and endogenous uncertainties," *IEEE Trans. on Power Systems*, 2021.

[23] J. Dupacová, "Optimization under exogenous and endogenous uncertainty," *University of West Bohemia in Pilsen*, 2006.

[24] CAISO, "Demand response issues and performance." [Online]. Available: http://www.caiso.com/participate/Pages/Load/Default.aspx.

[25] Z. Li, Q. Guo, and et al., "Sufficient conditions for exact relaxation of complementarity constraints for storage-concerned economic dispatch," *IEEE Trans. on Power Systems*, vol. 31, no. 2, pp. 1653–1654, 2015.

[26] N. Qi, "Supporting ges data and transformation brief." [Online]. Available: https://data.mendeley.com/datasets/8gm58ybsvg/draft?a=ba923181-51cf-4cd2-896e-b2095fc1c0be

[27] T. Homem-de Mello and G. Bayraksan, "Monte carlo sampling-based methods for stochastic optimization," *Surveys in Operations Research and Management Science*, vol. 19, no. 1, pp. 56–85, 2014.

[28] L. Herre, P. Pinson, and S. Chatzivasileiadis, "Reliability-aware probabilistic reserve procurement," *arXiv preprint arXiv:2110.11445*, 2021.

[29] C. T. Kelley, *Iterative methods for optimization*. SIAM, 1999.

[30] E. Roos, R. Brekelmans, and et al., "Tight tail probability bounds for distribution-free decision making," *European Journal of Operational Research*, vol. 299, no. 3, pp. 931–944, 2022.